ELSEVIER

Materials Science and Engineering A 375–377 (2004) 150–156

MATERIALS SCIENCE & ENGINEERING A

www.elsevier.com/locate/msea

Structure-forming principles for amorphous metals

D.B. Miracle [a,*], O.N. Senkov [b], W.S. Sanders [a], K.L. Kendig [a]

[a] *Materials and Manufacturing Directorate, Air Force Research Laboratory, Wright-Patterson AFB, OH, USA*
[b] *UES, Inc., 4401 Dayton-Xenia Road, Dayton, OH, USA*

Abstract

The purpose of this research is to establish structure-forming principles that govern the atomic structures of metallic glasses. A structural model based on efficient atomic packing will be discussed and applied to the topological systems that represent most metallic glass alloys. The concept of efficient atomic packing has direct and specific implications regarding the local structure and composition of metallic glasses. Specific solute-to-solvent atomic radius ratios and specific solute concentrations related to these ratios are shown to be preferred in this model, and analysis of a wide range of metallic glass systems shows a very strong correlation with these predicted values. Relationships between atomic size and concentration are discussed, and new insights are proposed based on the current structural model. Possible local atomic configurations (i.e., atomic clusters) are defined based on topological constraints that are derived from the requirement of efficient atomic packing. Experimental observations drawn from the literature that provide support for this model are presented.

Keywords: Structure; Atomic clusters; Amorphous metals

1. Introduction

A number of structural theories have been developed for the formation of glasses [1,2]. The most widely known theory is attributed to Zachariason [3] and provides four rules that describe the formation and linking of characteristic coordination polyhedra. This model offers a robust framework for describing the structure of oxide glasses, including those based on silicates, borates and phosphates. Bonding in these materials includes significant amounts of ionic (non-directional) and covalent (directional) bonds. Less-known structural theories include Sun's single bond strength criterion [4], based on bond strength, and Dietzel's field strength criterion [5], based on the magnitude of electrostatic interaction. More recently, a structural theory has been developed for chalcogenide glasses [6]. Based on topological considerations, this model provides insights into glasses formed in solids that are dominated by covalent bonding. The structures formed in all of these glass systems are relatively inefficiently packed due to constraints arising from preferred bond angles in solids with a significant covalent character and from constraints that arise from the requirement to maintain charge neutrality in ionic solids. Thus, the coordination number (N) is low in these glass systems and is generally less than ~8.

In contrast, cohesion in metallic glasses is dominated by metallic bonding. Although covalent bonding is sometimes suggested for metal–metalloid [7] and Al–transition metal (TM) [8,9] glasses, it has been argued that strong covalent bonding is difficult to rationalize for the metal–metalloid glasses due to the large coordination numbers (8–9) and the absence of boron d-orbitals [1]. By removing constraints introduced by preferred bond angles in covalent solids and, to a lesser extent, local charge neutrality in ionic solids, atomic packing in metallic glasses can be very efficient. Thus, atomic packing in crystalline metals is generally higher than in solids with a significant degree of covalent bonding, such as silicon and diamond. Furthermore, the density of the best metallic glasses is an exceptionally high fraction (~0.995) of the density of the same alloy in the crystalline state [10,11]. As a result, N in metallic glasses is rarely less than 8, and can be as large as 17 [12]. In spite of theories based on randomness as a structural paradigm for metallic glasses, significant short-range chemical and topological ordering is common in metallic glasses (see, for example, [9,13,14]). The general features described here for the structure of metallic glasses persist even in glasses with a small amount of covalent bonding in addition to metallic bonding. Thus,

* Corresponding author. Tel.: +1-937-255-9833; fax: +1-937-255-3007.
E-mail address: daniel.miracle@wpafb.af.mil (D.B. Miracle).

0921-5093/$ – see front matter © 2003 Elsevier B.V. All rights reserved.
doi:10.1016/j.msea.2003.10.130

a structural theory for the formation of metallic glasses that is able to explain the important structural distinctions of coordination number and atomic packing efficiency relative to oxide and chalcogenide glasses is required.

Earlier efforts to develop a structural theory for metallic glasses have considered concepts built upon a dense random packing (DRP) paradigm. Efforts to rationalize the high relative density of glasses in the amorphous structure relative to the same alloy composition in the crystalline state ($\rho_{rel} = \rho_{amor}/\rho_{xtal}$) have emphasized placement of solute atoms in the inefficiently packed local regions ('holes') that characterize a DRP array of spheres [15–17]. Careful analyses have shown that these approaches do not provide quantitative agreement with the high ρ_{rel} of metallic glasses [17–19]. A different approach, based on a continuous linked array of randomly arranged trigonal prismatic clusters in metal–metalloid glasses, has been proposed but has not been fully developed [13].

The purpose of this manuscript is to summarize and discuss recent developments in the establishment of structure-forming principles that govern the atomic structure of metallic glasses. Efforts to establish a structural paradigm based on efficient atomic packing will be described, and the influence of system topology (relative sizes and concentrations of constituent atoms) on local atomic configurations will be discussed. Initial models have emphasized the relative sizes of constituent atoms. The primary metrics used to determine the validity of these models will include consistency with widely accepted physical principles, an ability to explain the basic features for metallic glasses described above, and agreement with relevant experimental observations related to the formation of metallic glasses. It is anticipated that establishment of such principles will provide an improved understanding of the stability of metallic glasses, and may lead to a new structural theory for the formation and stability of metallic glasses.

2. The principle of efficient atomic packing

As described above, the best metallic glasses possess a high density relative to the crystalline state of the same alloy, which suggests that efficiently packed atomic configurations must be common features in the amorphous structure. From a kinetic perspective, an efficiently packed atomic structure is expected to provide higher viscosity relative to a more open structure. This increased viscosity reduces the rate of mass transport, and hence restricts nucleation and growth of competing crystalline phases. From an energetic perspective, a decrease in system volume decreases system energy, thus stabilizing the amorphous structure relative to competing structures. Consistent with this concept, evidence shows that metallic glass alloys often display a minimum in molar volume at the best glass forming composition [20,21]. Thus, the general concept of efficient atomic packing has a sound physical basis that is consistent with both energetic and kinetic models of metallic glass formation. While a structural model based on efficient atomic packing must consider a range in relevant length scales, the present developments will emphasize local packing efficiency on a length scale of a few atomic diameters. In the following section, the influence of relative atomic size on local packing efficiency will be described.

3. Influence of relative atomic size

A simple model is presented here to establish the influence of relative atomic size on local packing efficiency and to quantify local packing efficiency. This will be described briefly in two dimensions (2D), and will then be extended to three dimensions (3D). Consider a single circle surrounded by N equally sized larger circles, with a radius ratio R between the central (solute) and outer (solvent) circles. If R is selected so that there are no gaps between the circles in the first coordination shell, then it can be seen that this is qualitatively an efficiently packed configuration. If the central circle is enlarged slightly, then R increases and N remains unchanged, but gaps are formed between the solvent circles, forming a less efficiently packed configuration. As R continues to increase, the gaps between solvent circles continue to increase, producing a continuing decrease in packing efficiency (P). Eventually, a value of R is reached where an efficiently packed configuration with $N' = N + 1$ is once again achieved. A simple relationship between R and the theoretical coordination number (N^T) is given as [22]

$$N^T = \frac{\pi}{\arcsin(1/(1+R))} \tag{1}$$

N^T is a real number where the integer portion represents the number of full coordinating circles, N, and the fractional portion is a quantitative measure of the gaps between the circles in the first coordination shell. P may then be defined as the actual value of N normalized by N^T. It can be seen from this discussion that the local packing efficiency in 2D will reach a maximum value of unity at those specific values of R where N^T is an integer.

A similar analysis has recently been extended to 3D by deriving a solution for N^T that describes the number of equal-sized (solvent) spheres that can fit around a central (solute) sphere [19]. This represents a solute-centered atomic cluster with solvent atoms only in the first coordination shell. The result is given as [19]

$$N^T = \frac{4\pi}{\pi(2-q)+(2q)\arccos\{(\sin\pi/q)[1-1/(R+1)^2]^{1/2}\}} \tag{2}$$

where q is the maximum number of solvent atoms in the first coordination shell that can contact a given solvent atom that is also in the first coordination shell. The q value depends explicitly on R and is 3, 4 or 5. N may be determined experimentally from diffraction data, or may be calculated as the

Table 1
Values of N and corresponding values of R^*

N	R^* (Eq. (2))	R^* (cluster)	N	R^* (Eq. (2))	R^* (cluster)
3	0.155[a]	0.155	12	0.902	0.902
4	0.225	0.225	13	0.976	ND
5	0.362	Not stable	14	1.047	ND
6	0.414	0.414	15	1.116	ND
7	0.518	0.591	16	1.183	ND
8	0.617	0.645	17	1.248	ND
9	0.710	0.732	18	1.311	ND
10	0.799	0.834	19	1.373	ND
11	0.884	0.902	20	1.433	ND

[a] Calculated from Eq. (1). ND: not determined.

truncated value of N^T. In a hard sphere cluster, such as those described in the following section, N is the number of full spheres in the first coordination shell. P may be determined in 3D by truncating N^T in Eq. (2) and dividing by N^T. As described for the 2D example, a maximum P is obtained for specific values of R where N^T is an integer, designated as R^*. These values are given in Table 1 for a range in R that is most relevant for metallic and oxide glasses. Additional details relating to the derivation of these values is given in [19].

Thus, if efficient atomic packing in the first coordination shell is important in the formation of metallic glasses, then glasses should show a preference for these solute-to-solvent atom radius ratios. A large number of binary and complex metallic glass systems has been analysed [19] to explore a possible correlation between actual atomic radius ratios in reported metallic glasses and the predicted values of R^* in Table 1. One radius ratio ($R = r_{solute}/r_{solvent}$), representing solute-centered clusters with solvent atoms only in the first coordination shell, was determined for each of 76 binary metallic glasses. Complex metallic glass alloys based on Al, Au, Fe, La, Mg, Nd, Ni, Pd, Pt, Si, Sm, Ti and Zr were also included in this analysis. One radius ratio was determined for each solute in a given alloy family. For example, five values of R were determined from the Zr–Ti–Al–Cu–Ni–Be metallic glass system—one R for each of the five solutes. While atomic radii depend upon local structure and chemistry, differences are generally small in systems where metallic bonding dominates. Important differences from handbook values for metallic radii exist in some systems, including Al–TM glasses and glasses containing metalloids such as B, C, or P. The atomic radii used in the present analysis were taken from a critical assessment that accounts for these differences [23]. Additional details of this analysis of the correlation between solute radius ratios and predicted values of R^* is provided in [19].

A summary histogram showing the frequency with which particular radius ratios occur within these metallic glasses is shown in Fig. 1 [19]. The vertical lines represent the values of R^* calculated from Eq. (2). A strong correlation is shown for each class of metallic glass, and for all metallic glasses taken together. Although not yet rigorously analysed, initial observations of solute-to-solvent radius ratios in representative silicate and borosilicate oxide glasses also show a correlation with the predicted values of R^* [19], as do heavy metal fluoride glasses. Based on the strength of these correlations, it is concluded that the model for efficient atomic packing in the first coordination shell is a reasonable physical representation of the local atomic structure in metallic glasses.

A primary feature of this model is the presence of solvent atoms only in the first coordination shell. This is an accurate representation of the structure of silicate and borosilicate glasses. In addition, there is essentially no metalloid–metalloid bonding in metal–metalloid glasses [14,24], so that this model also fairly represents these well-known metallic glass systems. While significant short-range chemical ordering is a common feature in many metallic glasses, some degree of solute–solute bonding will be expected in metallic glasses. Where data is available, in fact, some solute–solute bonding has been observed [12,25–29]. Further, the present model provides a hard sphere idealization with no distortion in solute-solvent bonds. In spite of these details, the strong correlation between predicted radius ratios and those commonly observed in a diverse range of metallic glass systems suggests that these deviations in real systems from the model idealization may represent only a small correction to the model summarized here.

3.1. Characteristic atomic configurations

The model summarized in the preceding section is based on the maximum number of solvent atoms that *may* exist in the first coordination shell of a given solute atom. This is accomplished by determining the minimum area on a solute atom surface that is associated with (or 'occupied by') a solvent atom in the first coordination shell. The total surface area of the solute atom is divided by this minimum area associated with a single solvent atom to determine N^T. However, the actual area associated with a solvent atom is sometimes larger than this minimum value. For example, an octahedron exhibits $N = 6$ for $R = 0.414$, and only equilateral triangular faces are produced by connecting all of the vertices. This represents the most efficient packing around the central solute atom. On the other hand, a trigonal prism also possesses $N = 6$, but $R = 0.528$ and the faces of this polyhedron consist of two equilateral triangles and three squares. The three square faces indicate a less efficient packing, so that the surface area of the central atom associated with each of the atoms in the first coordination shell is larger than for the octahedron. This larger surface area associated with each solvent atom results in a larger R for the trigonal prism configuration relative to the octahedron. Thus, the actual value of R required to support a given value of N also depends upon geometrical constraints arising from packing of the solvent spheres in the first coordination shell. As a result, the actual atomic configurations must be specified to accurately determine the relationship between R and N. Stated differently, a given value of N

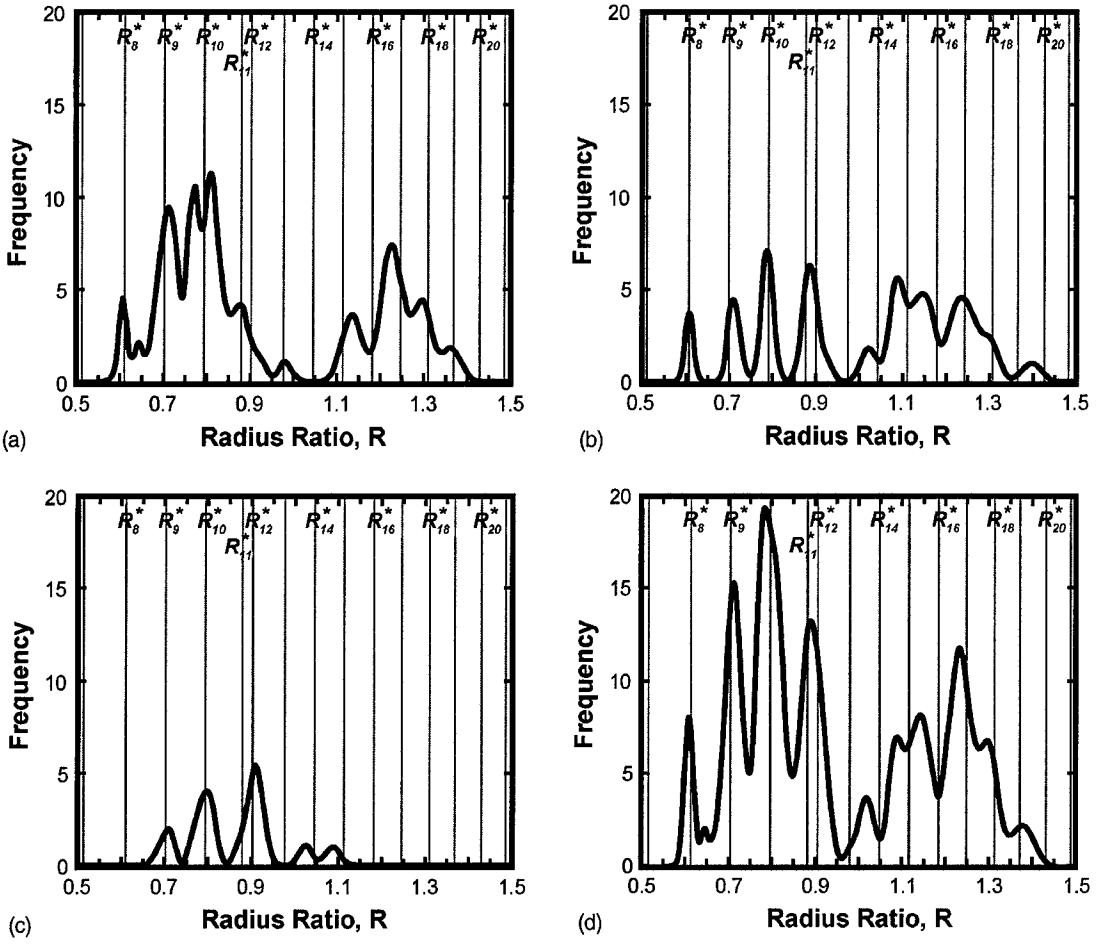

Fig. 1. Histograms displaying the correlation between predicted radius ratios (R^*), shown as vertical lines in the figures, and solute-to-solvent radius ratios observed in (a) binary metallic glasses, (b) metallic glasses with marginal glass forming ability and (c) bulk metallic glasses. A summation of these three plots is shown in (d) [19].

may be produced by several values of R, depending on the actual configuration of atoms in the first coordination shell. Alternatively, N^T represents an idealized configuration, so that a unique value of N^T is obtained for a given value of R.

Consideration of local atomic configurations is generally based on polyhedra that are common in crystalline or quasicrystalline solids, with $N = 4$, 6, 8 or 12. In addition, a capped trigonal prism with $N = 9$ has been established as a representative cluster in metal–metalloid glasses [13]. In metallic glasses, values of R are rarely smaller than ~0.6, so that $N \geq 8$ (see Table 1). Thus, atomic clusters with $N = 10$ or 11 may exist in metallic glasses with appropriate values of R, but the atomic configurations possible for these values of N are not yet established. Further, inspection of clusters with $N = 8$ from crystalline solids suggests intuitively that other more efficiently packed configurations may be possible. Relatively little work has been reported for clusters that are likely in systems with $R > 1$. In Frank–Kasper phases, atomic clusters with $N = 14$, 15 or 16 have been described in detail and have relevance in topologically close packed structures [30,31]. However, these clusters were constructed with constraints that may not represent the most efficiently packed configurations. Further, solutes with R as large as 1.4 are often observed in metallic glasses, so that clusters with N as large as 19 may be relevant in metallic glasses.

A systematic effort to explore and establish the actual atomic configurations that may exist for $8 \leq N \leq 19$ is now underway, and the initial observations are presented here. More than one configuration exists for most values of N, and these different configurations result in a range of R values for a given N. For example, six distinct cluster configurations have been constructed with $N = 10$, and corresponding values of R range from 0.834 to 0.902. Only stable configurations are considered, defined here as one where all equal-sized spheres in the first coordination shell just touch the central sphere, and each sphere in the first coordination shell touches at least three other spheres in the first shell. After constructing possible clusters, R can be calculated for each specific configuration from geometric analysis. The minimum value of R for each value of N provides a cluster-based determination of R^*, representing the most efficiently packed configuration for that value of N. The cluster-based values for R^* determined in this way are shown in Table 1, along with the values calculated from Eq. (2).

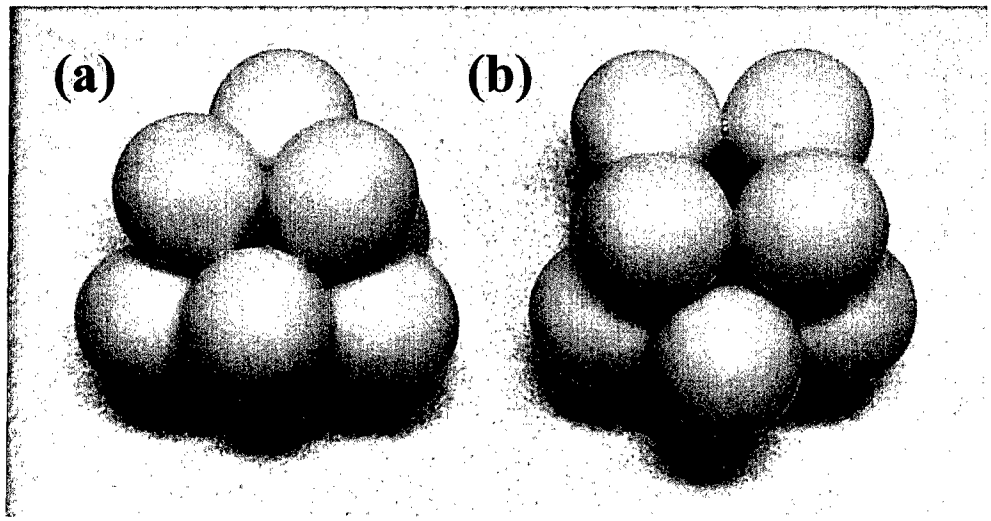

Fig. 2. Candidate clusters with high packing efficiency: (a) a distorted capped trigonal prism with $N = 9$ and $R = 0.732$, and (b) a cluster with $N = 10$ and $R = 0.834$.

Cluster-based values of R^* for $N = 3$, 4, 6 and 12 match the idealized predictions of Eq. (2) exactly. With the exception of the cluster for $N = 7$, the remaining actual clusters with $N < 12$ have values of R^* that are less than 5% higher than the ideal values predicted from Eq. (2). Studies in the mathematics community have provided rigorous solutions for the minimum value of R required for $2 \leq N \leq 12$ (see Table 11.1 in [32]). The results of these efforts match the cluster-based values of R^* in Table 1 to four significant digits, validating this cluster-based approach for determining values of R^*. The most efficiently packed cluster for $N = 8$ is a square antiprism and for $N = 11$ is an icosahedron with one sphere removed from the first coordination shell. Efficiently packed clusters with $N = 9$ and 10 are shown in Fig. 2. The cluster with $N = 9$ is a capped trigonal prism that has been extended along the prism axis to allow the three 'capping' atoms to contact the solute sphere as first nearest neighbors [33]. This configuration is stable for $R = 0.732$, whereas the trigonal prism is stable for $R = 0.528$. These larger values of R allow the distorted capped trigonal prism to dominate in metal–metalloid glasses, where the solute-to-solvent radius ratios range from 0.609 to 0.781 [33].

A systematic investigation of configurations that will produce a minimum value of R for $13 \leq N \leq 19$ is also suggested to be of interest with respect to possible atomic configurations in metallic glass structures. Initial work suggests that the differences in cluster-based values of R^* and those from Eq. (2) may be more significant than for $N > 12$. While there may be some interest in simply defining such configurations from a fundamental perspective, it is also important to identify approaches for determining whether such configurations actually occur in metallic glasses. Critical observations in diffraction experiments may provide some evidence, and careful analysis of atomistic simulations may also provide insight and support for such configurations.

Possible idealized local atomic configurations may be defined in a particular alloy system by considering efficiently packed clusters that may occur at the particular radius ratios exhibited by that alloy system. Support for the presence of such local configurations may be explored by comparing model predictions based on coordination numbers and measurement of local packing efficiency with experimental data. This approach has recently been pursued in Al–Y and Al–Y–Ni glass alloys [34]. The results of this initial study are consistent with the experimental data, so that the basic features of this model may be relevant in the actual metallic glass. However, further investigation is required to provide more convincing evidence for the validity of this model. Additional investigations may include comparisons with higher quality diffraction data than those currently available in the literature and may also include analysis of atomic simulations. Such efforts are now underway.

4. Influence of relative atomic concentration

Earlier efforts to establish the importance of atomic concentrations of constituent atoms on glass stability have focused on the relationship between atomic size and atomic concentration. A well-known model [23] provides an explicit relationship relating the volume difference between solute and solvent atoms and the minimum solute concentration required to destabilize the competing binary crystalline phase. This model gives an inverse relationship between R and the critical solute concentration in binary glasses, and provides a remarkably good ability to predict the critical solute concentration for a significant number of binary metallic glasses.

A phenomenological approach for visualizing and comparing the topology of binary and complex metallic glasses has recently been devised by plotting the atomic concentration and the atomic size relative to the solvent atom for

each element in a metallic glass [35]. These atomic size distribution plots (ASDPs) have been constructed for a large number of binary [33] and complex [35,36] metallic glasses. While ASDPs for most metallic glasses produce a profile of R versus concentration that is consistent with Egami's model, most of the best metallic glasses show a relationship where solute concentration increases as R decreases below a value of 0.8–0.9. Similarly, the most concentrated solute in silicate glasses (Si) is generally the smallest solute. Egami's model is not expected to predict the detailed profiles represented in ASDPs, since the former is developed for binary glasses only while ASDPs of BMGs represent complex metallic glasses where each of the constituents have been optimised to improve glass formability. Nevertheless, the inability of Egami's model to represent the general trend in the relationship between concentration and atomic size suggests that some fundamental physical feature may be missing from this model.

While Egami's model considers only substitutional occupancy for solute atoms, recent modifications consider that solute atoms may occupy either substitutional or interstitial sites in the competing crystalline lattice [37,38]. For $R < 0.81$, interstitial occupancy is energetically favored (produces a smaller strain energy) over placing the same solute in a substitutional site [38]. Further, as R becomes increasingly smaller than 0.81, the strain associated with an interstitial solute becomes increasingly smaller, so that the critical concentration increases with increasing difference between solute and solvent atom size for $R < 0.81$. This modification provides a physical basis for the composition trends observed in ASDPs for the most stable metallic glasses. Application of this modified model also provides a reasonable ranking of glass forming ability in complex metallic glasses [38]. However, additional work is still required to allow this model to rigorously account for the addition of several solutes in a single alloy.

Multicomponent amorphous alloys that contain both larger and smaller substitutional solutes relative to the solvent are generally more stable than binary amorphous alloys. This feature may be important for stabilization of the amorphous structure. Indeed, as substitutional atoms, the smaller atoms produce compressive lattice strains and the larger atoms produce tensile strain in the competing crystalline matrix. These opposite strain fields may attract each other, thereby reducing internal stresses and forming relatively stable short-range ordered configurations (clusters). If these clusters can be systematically linked to produce a structure with long-range crystalline symmetry, their formation will stabilize the crystal and make amorphization more difficult. However, if the short-range ordered clusters cannot be linked to produce crystalline symmetry, their formation should favour amorphization. Analysis of diffraction data in $Al_{90}Y_{10}$ and $Al_{87}Y_8Ni_5$ has shown that there is an exceptionally strong interaction between Y and Ni atoms, and the elastic interaction described here is proposed to contribute significantly to this behavior [34]. The model based on atomic volume difference would predict a decrease in the glass formability of alloys with both larger and smaller solutes relative to the solvent, and so contradicts experience [37]. The interpretation provided here provides a physically reasonable explanation, although a more rigorous analysis is required to validate this viewpoint.

A completely different situation, that has however the same nature, can be considered if solutes present in the alloy are small enough to occupy interstitial sites in the competing crystalline lattice. Indeed, a higher concentration of an interstitial atom is required to reach a critical internal strain for destabilization of the crystal lattice (amorphization) when the atomic size of this atom decreases relative to the size of the solvent for $R < 0.81$, as discussed above. Producing a tensile lattice strain, these interstitial atoms will attract substitutional atoms that are smaller than the solvent atom and repulse substitutional atoms that are larger than the solvent atom. In the former case, dense and stable short-range order configurations may be produced, which may stabilize the amorphous state, while the latter case explains why bulk metallic glasses containing large amounts of small interstitial elements do not generally contain solutes with atomic sizes larger than the atomic size of the base element (solvent).

A separate approach to exploring the relationship between the concentration of atomic species and the structure of metallic glasses has recently been proposed [19]. This approach is based on the concept that solute-centered clusters may form common structural elements in metallic glasses, and that these elements are linked together to form the glass structure. Such a concept is consistent with the results of the previous section, where specific solute-to-solvent radius ratios favor the formation of atomic clusters with a predictable value of N. This concept is also consistent with the stereochemically defined model [1]. In fact, an early effort to construct a metallic glass structure from capped trigonal prisms showed some promise [13]. In the approaches described here for efficient atomic packing, it is reasonable to expect that a crude relationship may exist between atomic concentration and N. If a structure is comprised of solute-centered clusters, and if each solvent atom is bonded to two solutes, then [19]

$$C_j \approx N_{ij} \tfrac{1}{2}(C_i) \tag{3}$$

where C denotes atomic concentration and the subscripts i and j represent solute and solvent atoms, respectively. This relation is satisfied for silicate glasses based on SiO_2 ($C_i = 0.33$ and $N_{ij} = 4$). Further, this model also provides a very good representation of metal–metalloid glasses, such as Ni–B, Fe–B and Co–P, where each solvent atom is coordination with ~2 metalloid atoms [39–41], and $C_i \sim 0.18$–0.2 and $N_{ij} \sim 8.5$–9. In Al–rare earth (RE) glasses, the critical RE atom fraction ranges from 0.09 to 0.13 [42] and the value of N_{Y-Al} is 14.1 ± 1.5 [12]. Thus, this simple model gives the solvent concentration as $0.63 \leq C_j \leq 0.92$, which spans the experimentally determined range of $0.87 \leq C_j \leq 0.91$ [42]. Of course, as N becomes large it is not likely that each

solvent atom can be shared by more than one solute, so that the factor of 1/2 in the right-hand side of Eq. (3) may require modification. In fact, the value of N_{Al-Y} in $Al_{90}Y_{10}$ is 1.6 ± 0.2, and in $Al_{87}Y_8Ni_5$ is 1.2 ± 0.2 [12]. Nevertheless, this simple model is a first attempt to provide a crude ability to relate atomic concentrations to the structure of metallic glasses.

5. Concluding remarks

Structural models for metallic glasses based on a dense random packed paradigm are unable to account for the key experimental observation of high density of an amorphous alloy relative to the density of the same alloy in the crystalline state. A new model based on efficiently packed local atomic configurations has been proposed. Several key features of this model are summarized and discussed here. A preference for specific solute-to-solvent atomic radius ratios predicted by this model has been validated by a strong correlation with radius ratios in a wide range of known metallic glasses. A dependence of solute concentration on atomic size is also discussed in the framework of this efficient atomic packing model. Finally, specific idealized atomic configurations are being constructed that are consistent with this model, and validation of the occurrence of these configurations in actual structures is being pursued by consistency with available experimental and computational results.

Acknowledgements

The authors would like to acknowledge encouraging comments by Profs. W. Johnson and T. Egami, and Dr. R. Schwarz. This research was supported under the DARPA Structural Amorphous Metals Initiative (Dr. L. Christodoulou, Program Manager) and AFOSR Task 01ML05–COR (Dr. C. Hartley, Program Manager).

References

[1] P.H. Gaskell, Models for the structure of amorphous solids, in: J. Zarzycki (Ed.), Materials Science and Technology, vol. 9, 1991, pp. 175–278.
[2] A.K. Varshneya, Fundamentals of Inorganic Glasses, Academic Press, San Diego, CA, 1993.
[3] W.H. Zachariasen, J. Am. Chem. Soc. 54 (1932) 3841.
[4] K.-H. Sun, J. Am. Ceram. Soc. 30 (1947) 277.
[5] A. Dietzel, Z. Electrochem. 48 (1942) 9.
[6] J.C. Phillips, J. Non-Cryst. Sol. 34 (1979) 153.
[7] G.W. Tecza, J. Hafner, J. Non-Cryst. Sol. 202 (1996) 1.
[8] L. Zhang, Y. Wu, X. Bian, H. Li, W. Wang, S. Wu, J. Non-Cryst. Sol. 262 (2000) 169.
[9] H.Y. Hsieh, T. Egami, Y. He, S.J. Poon, G.J. Shiflet, J. Non-Cryst. Sol. 135 (1991) 248.
[10] A.R. Yavari, A. Inoue, Volume effects in bulk metallic glass formation, in: Materials Research Society, vol. 554, 1999, pp. 21–30.
[11] G.S. Cargill, J. Appl. Phys. 41 (1970) 12.
[12] E. Matsubara, Y. Waseda, A. Inoue, H. Ohtera, T. Masumoto, Z. Naturforsch. 44a (1989) 814.
[13] P.H. Gaskell, in: H. Beck, H.-J. Guntherodt (Eds.), Models for the Structure of Amorphous Metals, Springer-Verlag, Berlin, Germany, 1983, pp. 5–49.
[14] S. Steeb, P. Lamparter, J. Non-Cryst. Sol. 156–158 (1993) 24.
[15] D.E. Polk, Acta Metall. 20 (1972) 485.
[16] W.M. Visscher, M. Bolsterli, Nature 239 (1972) 504.
[17] H.J. Frost, Acta Metall. 30 (1982) 889.
[18] A.S. Clarke, J.D. Wiley, Phys. Rev. B 35 (1987) 7350.
[19] D.B. Miracle, W.S. Sanders, O.N. Senkov, Phil. Mag. A 83 (2003) 2409.
[20] P. Ramachandrarao, Z. Metallkunde 71 (1980) 172.
[21] O. Jin, R.B. Schwarz, F.M. Alamgir, H. Jain, in: A. Gonis, P.E.A. Turchi, A.J. Ardell (Eds.), Nucleation and Growth Process in Materials, vol. 580, MRS, Pittsburgh, PA, USA, 2000, pp. 277–283.
[22] T. Egami, Mater. Sci. Eng. A 226–228 (1997) 261.
[23] T. Egami, Y. Waseda, J. Non-Cryst. Sol. 64 (1984) 113.
[24] P. Lamparter, S. Steeb, Structure of amorphous and molten alloys, in: V. Gerold (Ed.), Structure of Solids, vol. 1, Materials Science and Technology, A Comprehensive Treatment, VCH, Weinheim, Germany, 1993, pp. 217–288.
[25] G.S. Cargill, in: Short-range Order in Amorphous GdFe2, American Institute of Physics, New York, NY, 1974, pp. 631–635.
[26] T. Fukunaga, N. Watanabe, K. Suzuki, J. Non-Cryst. Sol. 61–62 (1984) 343.
[27] P. Lamparter, S. Steeb, E. Grallath, Z. Naturforsch. 38a (1983) 1210.
[28] A. Lee, G. Etherington, C.N.J. Wagner, J. Non-Cryst. Sol. 61–62 (1984) 349.
[29] M. Maret, A. Soper, G. Etherington, C.N.J. Wagner, J. Non-Cryst. Sol. 61–62 (1984) 313.
[30] F.C. Frank, J.S. Kasper, Acta Cryst. 11 (1958) 184.
[31] F.C. Frank, J.S. Kasper, Acta Cryst. 12 (1959) 483.
[32] T. Aste, D. Weaire, The Pursuit of Perfect Packing, Institute of Physics, Bristol, UK, 2000.
[33] D.B. Miracle, J. Non-Cryst. Sol. 317 (2003) 40.
[34] D.B. Miracle, O.N. Senkov, J. Non-Cryst. Sol. 319 (2003) 174.
[35] O.N. Senkov, D.B. Miracle, Mater. Res. Bull. 36 (2001) 2183.
[36] D.B. Miracle, O.N. Senkov, in: S. Hanada, N. Masahashi (Eds.), Proceedings of the Fourth Pacific Rim International Conference on Advanced Materials and Processing (PRICM4), vol. II, The Japan Institute of Metals, Tokyo, Japan, 2001, pp. 2893–2896.
[37] T. Egami, J. Non-Cryst. Sol. 205–207 (1996) 575.
[38] O.N. Senkov, D.B. Miracle, J. Non-Cryst. Sol. 317 (2003) 34.
[39] E. Nold, P. Lamparter, H. Olbrich, G. Rainer-Harbach, S. Steeb, Z. Naturforsch. 36a (1981) 1032.
[40] J.F. Sadoc, J. Dixmier, Mater. Sci. Eng. 23 (1976) 187.
[41] P. Lamparter, W. Sperl, S. Steeb, J. Bletry, Z. Naturforsch. 37a (1982) 1223.
[42] A. Inoue, Prog. Mater. Sci. 43 (1998) 365.